Comparison of Causality Analysis on Simultaneously Measured fMRI and NIRS Signals during Motor Tasks*

Abdul Rauf Anwar**[1], Makii Muthalib[4], Stephane Perrey[3], Andreas Galka[5], Oliver Granert[2], Stephan Wolff[6], Guenther Deuschl[2], Jan Raethjen[2], Ulrich Heute[1] and Muthuraman Muthuraman[2]

***Abstract*— Brain activity can be measured using different modalities. Since most of the modalities tend to complement each other, it seems promising to measure them simultaneously. In to be presented research, the data recorded from Functional Magnetic Resonance Imaging (fMRI) and Near Infrared Spectroscopy (NIRS), simultaneously, are subjected to causality analysis using time-resolved partial directed coherence (tPDC). Time-resolved partial directed coherence uses the principle of state space modelling to estimate Multivariate Autoregressive (MVAR) coefficients. This method is useful to visualize both frequency and time dynamics of causality between the time series. Afterwards, causality results from different modalities are compared by estimating the Spearman correlation. In to be presented study, we used directionality vectors to analyze correlation, rather than actual signal vectors. Results show that causality analysis of the fMRI correlates more closely to causality results of oxy-NIRS as compared to deoxy-NIRS in case of a finger sequencing task. However, in case of simple finger tapping, no clear difference between oxy-fMRI and deoxy-fMRI correlation is identified.**

I. INTRODUCTION

Understanding the underlying functional connectivity in the brain is of vital importance. Detailed information about such connectivity will increase our knowledge about the signal flow between sources and sinks in the brain[1]. Different modalities have emerged in the recent past that measure brain activity directly (Electroencephalography (EEG)/ Magnetoencephalography (MEG)) or indirectly (Functional Magnetic Resonance Imaging (fMRI)/ Near Infrared Spectroscopy (NIRS)). Electroencephalography measures electric potentials by placing electrodes on the scalp. Such potentials originate from accumulative activity of millions of neurons. In magnetoencephalography, magnetometers are placed over the scalp to detect the magnetic field generated by the same number of neurons in the brain. Functional magnetic resonance imaging (fMRI) exploits the fact that neural activity in a specific part of the brain results in the increased demand of haemoglobin to that region. Blood with different concentration of oxygen reacts differently to the applied magnetic field resulting in the so-called BOLD (Blood oxygen level dependent) signal. fMRI can detect brain activity from subcortical areas successfully but it suffers from a low sampling rate. The principle of NIRS is based on monochromatic light absorption by haemoglobin, which can be used, indirectly, to estimate neural activation in the brain. Usually two lasers with different frequencies are used to estimate both oxy- and deoxy-haemoglobin. In order to identify signal source, principle of Granger causality can be used [2]. Directionality analysis using Granger causality based methods have been applied to fMRI data [3] [4]. In case of NIRS, such methods have been applied in animal [5] and human study [6]. In the following, we apply directionality analysis to simultaneously recorded fMRI and NIRS (both oxy and deoxy) time series and compare results from both using the statistical test of Spearman correlation.

*This work was supported by SFB 855 Project D2

[1]**A. R. Anwar and U. Heute are with the Faculty of Digital Signal Processing and System theory, University of Kiel, 24143 Kiel, Germany ara at tf.uni-kiel.de, uh at tf.uni-kiel.de

[2]M. Muthuraman, O. Granert, J. Raethjen and G. Deuschl are with the Department of Neurology, University of Kiel, 24105 Kiel, Germany m.muthuraman at neurologie.uni-kiel.de, o.granert at neurologie.uni-kiel.de, j.raethjen at neurologie.uni-kiel.de, g.deuschl at neurologie.uni-kiel.de

[3]S. Perrey is with Movement to Health (M2H), Euromov, Montpellier-1 University, 34090 Montpellier, France stephane.perrey at univ-montp1.fr

[4]M. Muthalib is with Movement to Health (M2H), Euromov, Montpellier-1 University, 34090 Montpellier, France and also with the Faculty of Health, Queensland University of Technology, 4059 Brisbane, Australia makii.muthalib at univ-montp1.fr

[5]A. Galka is with the Department of Neuropediatrics, University of Kiel, 24105 Kiel, Germany a.galka at pedneuro.uni-kiel.de

[6]S. Wolff is with the Department of Neuroradiology, University of Kiel, 24105 Kiel, Germany s.wolff at neurorad.uni-kiel.de

II. METHODS

Different methods to analyze the directionality between time series exist. The analysis of neurological time series is more meaningful in the frequency domain. So, investigation of causality between medical time series in the frequency domain seems pragmatic. Such methods include directed transfer function (DTF) [7], partial directed coherence (PDC) [8], modified directed transfer function (dDTF) [9], generalized partial directed coherence (gPDC) [10], and renormalized partial directed coherence (rPDC) [11]. All these methods are based on the principle of Granger causality that, in its original form, has also been applied to medical data, especially to fMRI data successfully [12] [13]. In this study we will use time-resolved partial directed coherence (tPDC), which has the additional advantage of not only giving frequency information about causal connections but also information about their time dynamics [14]. Assuming time series $x_j(t)$ is causing time series $x_i(t)$, we have:

$$x_i(t) = \sum_{r=1}^{P} a_{ij}(r) x_j(t-r) + \epsilon(t). \qquad (1)$$

Here, a_{ij} are the causal coefficients describing the behaviour

of causality from x_j to x_i. P is the maximum delay (optimum order) and ϵ is driving white noise. The coefficients of causality are of prime importance; they tell us whether causality exists between time series and also about its intensity if it exists. Using the Fourier transform of these coefficients, PDC from time series $x_j(t)$ to time series $x_i(t)$ can be calculated using the following formula [15]:

$$|\pi_{i \longleftarrow j}(w)| = \frac{|A_{ij}(w)|}{\sqrt{\sum_k |A_{kj}(w)|^2}}. \quad (2)$$

Causality from x_j to x_i can be interpreted as connection from x_j to x_i . Partial directed coherence shows the strength of the connection in the frequency domain. Calculation of the PDC is based on the estimation of causal coefficients, which are also called Multivariate Autoregressive (MVAR) coefficients. Number of these coefficients is defined by the optimum order, which can be estimated by fitting an appropriate Autoregressive (AR) model to the data and using Akaike's Information Criterion (AIC). During calculation of PDC, each coefficient is estimated by taking the whole time series into account. However, if we divide the time series into small segments and fit a model to each one separately, the PDC on each epoch can help us to visualize the time dynamics of causality. In order to calculate tPDC, we estimate MVAR coefficients at each time instance of the time series only taking into account a certain number of past values (optimum order). After finding these time-varying MVAR coefficients, PDC is calculated at each time point, and finally a time-frequency graph is plotted. In order to estimate time varying MVAR coefficients, we use the concept of state space modelling and model our time series by these two equations [16]:

$$x(k) = F[x(k-1), w] + Bv(k), \quad (3)$$

$$y(k) = Cx(k) + n(k). \quad (4)$$

For a linear model, $F[x(k)]$ can be written as $Ax(k)$. Both $v(k)$ and $n(k)$ can be assumed as Gaussian white noise. Time series $y(k)$ is the observed one, and our aim is to estimate $x(k)$. A and C are process and observation matrices, respectively. For non linear model, we have to estimate w too, and this can be done by approximating the non-linear function by a linear one which is varying in time [16]. In essence, at each time point, we estimate w and x. This gives us two Kalman filters running in parallel, hence named as *dual extended Kalman filter*(DEKF) [16]. In the present study DEKF is used on fMRI and NIRS data separately.

Before applying it to the medical data, the DEKF was tested to estimate the time varying coefficients on model data which were taken from [17]:

$$x_1(t) = 0.59x_1(t-1) - 0.2x_1(t-2) + a(t)x_2(t-1) + b(t)x_3(t-1) + \epsilon_1(t), \quad (5)$$

$$x_2(t) = 1.58x_2(t-1) - 0.96x_2(t-2) + \epsilon_2(t), \quad (6)$$

$$x_3(t) = 0.60x_3(t-1) - 0.91x_3(t-2) + \epsilon_3(t). \quad (7)$$

Here, the time-varying MVAR coefficients $a(t)$ and $b(t)$ have time dynamics as shown in Fig. 1.

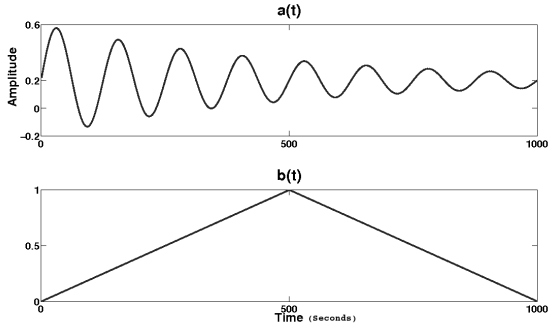

Fig. 1. Time varying coefficients: The upper plot shows dynamics of causal coefficient from x_2 to x_1, while the lower plot shows dynamics between x_3 and x_1.

After fitting the appropriate model to the data, time-varying PDC was calculated for this model. The results are shown in Fig. 2. We can see that the connections and the time dynamics were successfuly revealed by tPDC. Following the

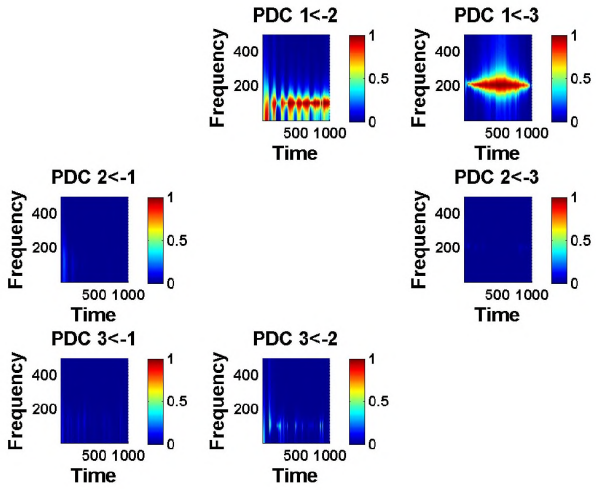

Fig. 2. Result of applying tPDC on model data. The two connections and their time dynamics have been successfully revealed. One can see that x_2 is causing x_1 in a sinusoidal way while connection from x_3 to x_1 follows a triangular shape over the course of time.

testing of this method on the model data, we applied it on medical data. For this purpose 6 healthy subjects (5 females and 1 male) were chosen to perform voluntary motor tasks using the right hand. The subject's mean age is 25 years (with standard deviation of 5 years). Prior to recording, all participants provided written consent. All subjects, except one, were right handed. Task details are as follows:

1. Finger tapping (FT): Simple tapping of index finger at approximately 2-5 Hz in a rhythmic fashion.
2. Simple finger sequencing (SFS): Sequential tapping of index, middle, ring and fourth finger against thumb.

The target area of finger motor tasks is within the scope of NIRS and fMRI measurement. The block design was used in

which the subjects were asked to perform the motor task for 30 seconds followed by 30 seconds rest. The total recording time was 600 seconds; hence 10 complete (activity-rest) blocks were obtained.

We used continuous-wave NIRS system (OXYMON MK-lll, Artinis, The Netherlands) measuring oxy-, deoxy- and total haemoglobin concentration in the blood by directing a monochromatic laser into the skull. The standard configuration with two wavelengths (856nm and 781 nm) per channels was used. The sampling rate was 10 Hz. Five detectors (avalanche photo diode) and 11 transmitters (pulsed laser diodes) were used to obtain 15 channels. The distance between each transmitter and detector was around 3.5 cm. MRI-compatible cables of length 10 meter were used to connect the NIRS monitoring/recording instrument with NIRS optodes during fMRI recording. The fMRI scanner (10 MHz output) was also synchronized with the NIRS system
BOLD-sensitive MRI was performed with a 3-Tesla MR scanner (Philips Achieva, Philips, Best, the Netherlands) and a standard, 8-channel SENSE head coil. A single-shot T1-weighted, gradient-echo planar imaging sequence was used for fMRI (TR = 2500 ms, TE = 45 ms, 32 slices, 64 x 64 matrix, slice thickness = 3.5 mm, FOV = 200 mm, flip angle = 90). The sampling rate was 2.5 seconds; hence, 240 brain volumes were acquired during the 600 seconds [18].

III. Results

Activation maps with 30 seconds motor task followed by 30 seconds of rest were constructed using the block design. In order to locate NIRS probes, fiduciary markers were placed between each transmitter and receiver pair so that the position of the NIRS channel can be located in fMRI plots. For each receiver, we used two NIRS time series (oxy and deoxy). Prior to any processing, a band-pass filter with cut off frequencies of 0.01 and 0.5 Hz was applied to both time series [19]. Afterwards, both time series were smoothed using a window length of 25 points. This process reduced the length of NIRS time series from 6000 to 240 data points. In case of fMRI, all scans were realigned, normalized and smoothed. The size of clusters was chosen as 5 voxels with P value of 0.01(corrected), and fMRI time series were extracted from three regions of the brain, namely, contralateral motor cortex (CMC), premotor cortex (PMC), and prefrontal cortex (PFC). A sphere with a radius of 3mm was assumed as source of activation in the desired part of the brain for time-series extraction [4]. All pre-processing of fMRI and time series extraction was performed using the SPM08 toolbox. (http://www.fil.ion.ucl.ac.uk/spm). Using the positions of fiduciary markers in fMRI, we made sure that we extract time series from specific parts of the brain which are exactly below the NIRS channels so that both time series can be compared. Region of interest around highest activation point was used in case of fMRI to compare it with NIRS. Out of 15 NIRS channels, only 3 were used. We did this because we are interested in only three regions of the brain. Each region of brain was covered by multiple NIRS probes. Position of NIRS probes was confirmed from activation maps of fMRI and using fiducial markers. Layout of selected probes is shown in Fig. 3. Colored four-cornered

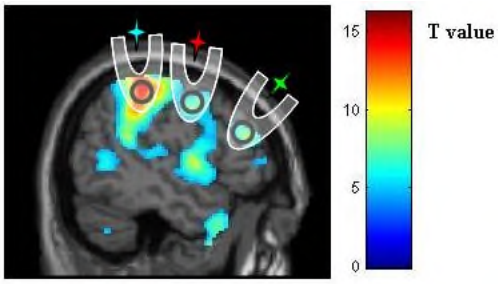

Fig. 3. Layout used for NIRS probes. Color stars show the approximate position of NIRS channel. Black circle, inside cortex show, corresponding fMRI ROI. Hypothetical banana curves between NIRS optodes are also shown

stars show the position of NIRS channels. Black circle inside the cortex show the location of respective ROI. The first and last data points of both NIRS(oxy and deoxy) and fMRI time series were discarded and tPDC was applied to all three time series (oxy-NIRS, deoxy-NIRS, and fMRI).

In the resulting time frequency plot, bins were created on the frequency axis and tPDC values inside a single bin were compared to tPDC values inside a similar bin in the other modality. Ten bins were created on the complete frequency axis (0 - 0.2 Hz) and tPDC magnitudes within each bin (0 - 0.02 Hz) are stored as a vector for further analysis. We did this because there is not much information on the frequency axis due to the very low sampling rate of fMRI, also NIRS time series were smoothed with window length of 25 data points, resulting in the same effective sampling rate as that of fMRI. Spearman correlation was calculated between time vectors (bin vectors) of oxy-NIRS and fMRI and also between deoxy-NIRS and fMRI. Positive significant correlation (value of $P<0.05$) between two time series (vectors in our case) shows that both time series are showing the same causal dynamics, a negative value meaning the opposite. Of all the significant connections we calculated the number of positive correlations and the number of negative correlations. Results are presented in Fig. 4. In addition to calculation of number of correlations, mean correlation (both positive and negative) along with standard error of mean was also calculated and shown in Fig. 5.

Results show that oxy-NIRS time series is more closely related to fMRI as compared to its deoxy counterpart in case of the finger-sequence task. In addition to an increased number of positive correlations, the number of negative correlations was also reduced during the finger-sequence task. During finger-tapping task, no clear difference was observed. It could be due to limited activation regions in the brain as can be seen from our own earlier study [18]. Better correlation of fMRI signal with oxy-NIRS is in accordance with published literature in this regard [19] [20]. This could be due to the observation that an increase in BOLD activity is accompanied by decrease in deoxy-NIRS during motor task [19]. However significance of our

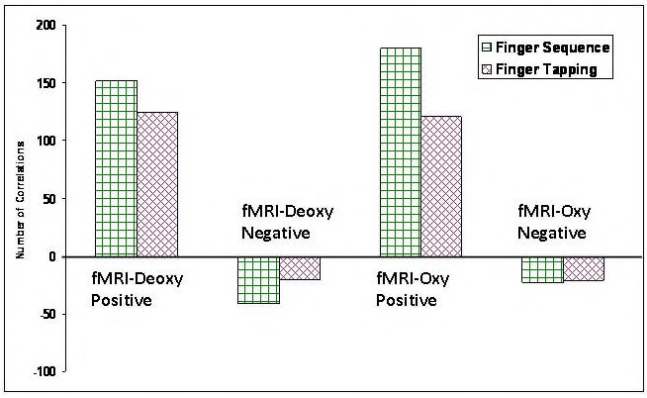

Fig. 4. Results showing that more number of positive correlations was between oxy-NIRS and fMRI as compared to deoxy-NIRS and fMRI in case of finger-sequence task. Number of negative correlations is also less in oxy-NIRS and fMRI as compared to deoxy-NIRS and fMRI. However incase of finger-tapping task, no clear difference is seen.

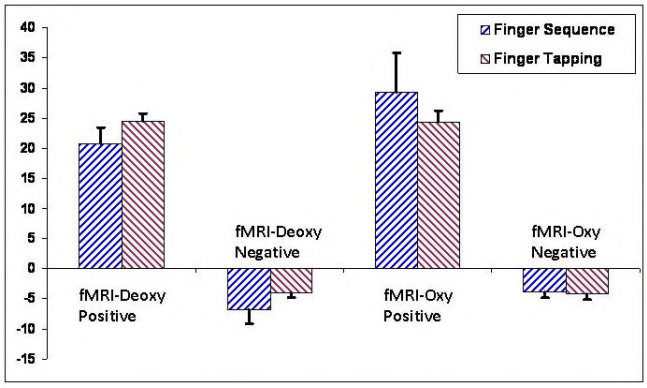

Fig. 5. Subject wise correlation measure is depicted in this figure. Increased number of positive correlations between fMRI and oxy-NIRS, along with increased number of negative correlations between fMRI and deoxy-NIRS are shown for both tasks. Standard error of mean are also indicated by bars

study is to analyze correlation of causality vectors instead of signal vectors. Our findings show that Granger-causality based methods can be applied to non invasive modalities like NIRS and have potential to be a promising tool for estimating underlying functional networks of the brain during voluntary and involuntary tasks.

ACKNOWLEDGMENT

Support from the German Research Council (Deutsche Forschungsgemeinschaft, DFG, SFB 855, Project D2) is gratefully acknowledged.

REFERENCES

[1] A. B. Barrett, M. Murphy, M. -A. Bruno, Q. Noirhomme, M. Boly, S. Laureys, A. K. Seth, Granger Causality Analysis of Steady-State Electroencephalographic Signals during Propofol-Induced Anaesthesia, PLoS One. 2012; 7(1): e29072. Published online January 5, 2012.

[2] C. W. J. Granger, Investigating Causal Relations by Econometric Models and Cross-spectral Methods. Econometrica, Vol. 37, Issue No. 3. August 1969, pp. 424-438.

[3] J. R. Sato1, D. Y. Takahashi, S. M. Arcuri, K. Sameshima, P. A. Morettin, L. A. Baccala, Frequency domain connectivity identification: An application of partial directed coherence in fMRI, Human Brain Mapping, Volume 30, Issue 2, pages 452-461, February 2009.

[4] L. Zhang, G. Zhong, Y. Wu, M. G. Vangel, B. Jiang, and J. Kong, Using Granger-Geweke causality model to evaluate the effective connectivity of primary motor cortex (M1), supplementary motor area (SMA) and cerebellum, J Biomed Sci Eng. 2010 September; Volume 3; Issue 9: pp 848-860.

[5] C. Im, Y. Jung, S. Lee, D. Koh, D. Kim, and B. Kim, Estimation of directional coupling between cortical areas using Near-Infrared Spectroscopy (NIRS), Opt. Express 18, 5730-5739 (2010).

[6] L. Holper, F. Scholkmann, M. Wolf, Between-brain connectivity during imitation measured by fNIRS, NeuroImage, Volume 63, Issue 1, October 2012, Pages 212-222.

[7] M.J. Kaminski and K.J. Blinowska, A new method of the description of the information flow in the brain structures. Biological Cybernetics, July 1991, Volume 65, Issue 3, pp 203-210.

[8] L. A. Baccala, K. Sameshima, Partial directed coherence: a new concept in neural structure determination. Biol Cybern. 2001 Jun; Volume 84; Issue 6: pp 463-74.

[9] A. Korzeniewska, M. Manczak, M. Kaminski, K. J. Blinowska, S. Kasicki, Determination of information flow direction among brain structures by a modified directed transfer function (dDTF) method, Journal of Neuroscience Methods, Volume 125, Issues 1-2, 30 May 2003, Pages 195-207.

[10] L.A. Baccald, F. de Medicina; Generalized Partial Directed Coherence, Digital Signal Processing, 2007 15th International Conference on, pp.163-166, 1-4 July 2007.

[11] B. Schelter, J. Timmer, M. Eichler, Assessing the strength of directed influences among neural signals using renormalized partial directed coherence, Journal of Neuroscience Methods, Volume 179, Issue 1, 30 April 2009, Pages 121-130.

[12] A. Gaglianese, M. Costagli, G. Bernardi, E. Ricciardi, P. Pietrini, Evidence of a direct influence between the thalamus and hMT+ independent of V1 in the human brain as measured by fMRI, NeuroImage, Volume 60, Issue 2, 2 April 2012, Pages 1440-1447.

[13] Y. Alkan, T. L. Alvarez, S. Gohel, P.A. Taylor, B.B. Biswal, Functional connectivity in vergence and saccade eye movement tasks assessed using Granger Causality Analysis, Engineering in Medicine and Biology Society,EMBC, 2011 Annual International Conference of the IEEE, pp.8114-8117, Aug. 30 2011-Sept. 3 2011.

[14] B. Schelter, L. Sommerlade, B. Platt, A. Plano, M. Thiel, J. Timmer, Multivariate analysis of dynamical processes with applications to the neurosciences, Engineering in Medicine and Biology Society,EMBC, 2011 Annual International Conference of the IEEE, pp.5931-5934, Aug. 30 2011-Sept. 3 2011.

[15] B. Schelter, M. Winterhalder, M. Eichler, M. Peifer, B. Hellwig, B. Guschlbauer, C. H. Lcking, R. Dahlhaus, J. Timmer, Testing for directed influences among neural signals using partial directed coherence, Journal of Neuroscience Methods, Volume 152, Issues 1-2, 15 April 2006, Pages 210-219.

[16] E. A. Wan, A. T. Nelson, Neural dual extended Kalman filtering: applications in speech enhancement and monaural blind signal separation, Neural Networks for Signal Processing [1997] VII. Proceedings of the 1997 IEEE Workshop, pp.466-475, 24-26 Sep 1997.

[17] L. Sommerlade, K. Henschel, J. Wohlmuth, M. Jachan, F. Amtage, B. Hellwig, C. H. Lcking, J. Timmer, B. Schelter, Time-variant estimation of directed influences during Parkinsonian tremor, Journal of Physiology-Paris, Volume 103, Issue 6, November 2009, Pages 348-352.

[18] A.R. Anwar, M. Muthalib, S. Perrey, A. Galka, O. Granert, S. Wolff, G. Deuschl, J. Raethjen, U. Heute, M. Muthuraman, Directionality analysis on functional magnetic resonance imaging during motor task using Granger Causality, Engineering in Medicine and Biology Society (EMBC), 2012 Annual International Conference of the IEEE, pp.2287-2290, Aug. 28 2012-Sept. 1 2012

[19] X. Cui, S. Bray, D. M. Bryant, G. H. Glover, A. L. Reiss, A quantitative comparison of NIRS and fMRI across multiple cognitive tasks, NeuroImage, Volume 54, Issue 4, 14 February 2011, Pages 2808-2821.

[20] J. Steinbrink, A. Villringer, F. Kempf, D. Haux, S. Boden, H. Obrig, Illuminating the BOLD signal: combined fMRI-fNIRS studies, Magnetic Resonance Imaging, Volume 24, Issue 4, May 2006, Pages 495-505.